

See discussions, stats, and author profiles for this publication at: <https://www.researchgate.net/publication/51518974>

Stability Effects on CO₂ Adsorption for the DOBDC Series of Metal–Organic Frameworks

ARTICLE *in* LANGMUIR · AUGUST 2011

Impact Factor: 4.46 · DOI: 10.1021/la201774x · Source: PubMed

CITATIONS

65

READS

199

6 AUTHORS, INCLUDING:



Jian Liu

Pacific Northwest National Laboratory

35 PUBLICATIONS 1,341 CITATIONS

SEE PROFILE



Richard Willis

Honeywell

34 PUBLICATIONS 1,335 CITATIONS

SEE PROFILE

Stability Effects on CO₂ Adsorption for the DOBDC Series of Metal–Organic Frameworks

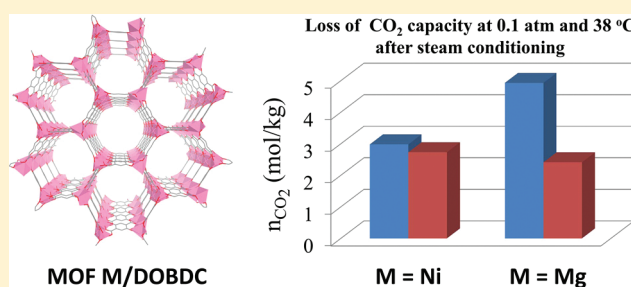
Jian Liu,[†] Annabelle I. Benin,[‡] Amanda M. B. Furtado,[†] Paulina Jakubczak,[‡] Richard R. Willis,[‡] and M. Douglas LeVan^{*,†}

[†]Department of Chemical and Biomolecular Engineering, Vanderbilt University, VU Station B 351604, Nashville, Tennessee 37235-1604, United States

[‡]UOP LLC, a Honeywell Company, Des Plaines, Illinois 60017, United States

 Supporting Information

ABSTRACT: Metal–organic frameworks with unsaturated metal centers in their crystal structures, such as Ni/DOBDC and Mg/DOBDC, are promising adsorbents for carbon dioxide capture from flue gas due to their high CO₂ capacities at sub-atmospheric pressures. However, stability is a critical issue for their application. In this paper, the stabilities of Ni/DOBDC and Mg/DOBDC are investigated. Effects of steam conditioning, simulated flue gas conditioning, and long-term storage on CO₂ adsorption capacities are considered. Results show that Ni/DOBDC can maintain its CO₂ capacity after steam conditioning and long-term storage, whereas Mg/DOBDC does not. Nitrogen isotherms for Mg/DOBDC show a drop in surface area after steaming, corresponding to the decrease in CO₂ adsorption, which may be caused by a reduction of unsaturated metal centers in its structure. Conditioning with dry simulated flue gas at room temperature only slightly affects CO₂ adsorption in Ni/DOBDC. However, introducing water vapor into the simulated flue gas further reduces the CO₂ capacity of Ni/DOBDC.



1. INTRODUCTION

Adsorption is a promising technique for capturing carbon dioxide from flue gas because of its efficiency and low energy requirement.^{1,2} Metal–organic frameworks (MOFs) are novel adsorbents for gas adsorption with high surface areas, large pore volumes, and a wide diversity of structures and compositions.^{3–9} Millward et al.¹⁰ showed that some MOFs have larger saturated CO₂ capacities than traditional zeolites at room temperature and 42 bar. While this is useful for storage or high pressure separation, the partial pressure of CO₂ in a typical flue gas is about 0.1 atm.

Many researchers have studied CO₂ adsorption in MOFs at subatmospheric pressures. Yazaydin et al.¹¹ used both experiments and simulation to screen MOFs for the highest CO₂ capacities at about 0.1 atm. They found that Mg/DOBDC and Ni/DOBDC have the highest CO₂ capacities at 0.1 atm for the 14 MOFs that they considered. Britt et al.¹² reported that Mg-MOF-74 (i.e., Mg/DOBDC) has 8.9 wt % dynamic capacity for CO₂ adsorption while requiring only a mild regeneration process. Their results demonstrated the potential of using the DOBDC series of MOFs with open metal sites (i.e., unsaturated metal centers) as efficient CO₂ capture adsorbents. Bao et al.¹³ showed that Mg-MOF-74 has a similar adsorption selectivity between CO₂ and CH₄ but much higher adsorption capacities for CO₂ and CH₄ compared to NaX zeolites.

The structural units of the DOBDC series of MOFs are constructed with metal centers (Zn, Ni, Co, or Mg) and 2,5-dihydroxyterephthalic acid (2,5-dihydroxybenzenedicarboxylic

acid, DOBDC) molecules as shown in Figure 1. Both the aryloxy and carboxylate functionalities of the DOBDC ligand bind to the metal ion centers. The DOBDC series of MOFs has 1D pores with a uniform pore size of 11 Å after removal of solvent molecules.¹⁴ According to the literature, MOFs with different metal centers in the DOBDC series have quite different CO₂ capacities under the same conditions. Metal substitution in the DOBDC series can impact the CO₂ capacity significantly.¹⁵ This effect may be caused by the difference in the ionic character of the metal–oxide bonds in the DOBDC-series of MOFs.^{11,15}

MOFs in the DOBDC series have drawn considerable attention because of unsaturated metal centers (UMCs) in their structures, which are essential for CO₂ adsorption at subatmospheric pressures. However, as pointed out by Keskin et al.¹⁶ in their recent review, data regarding coadsorption of water and CO₂ in MOFs and their stabilities toward low temperature steam is urgently needed for research on using MOFs in large scale CO₂ separations.

In our previous paper in this journal, CO₂/H₂O coadsorption data were reported for HKUST-1 and Ni/DOBDC.¹⁷ Those two MOFs were selected as examples from over 30 MOFs that we have considered, among which Mg/DOBDC has the highest CO₂ capacity and Ni/DOBDC has the second highest CO₂

Received: May 11, 2011

Revised: July 25, 2011

Published: July 25, 2011

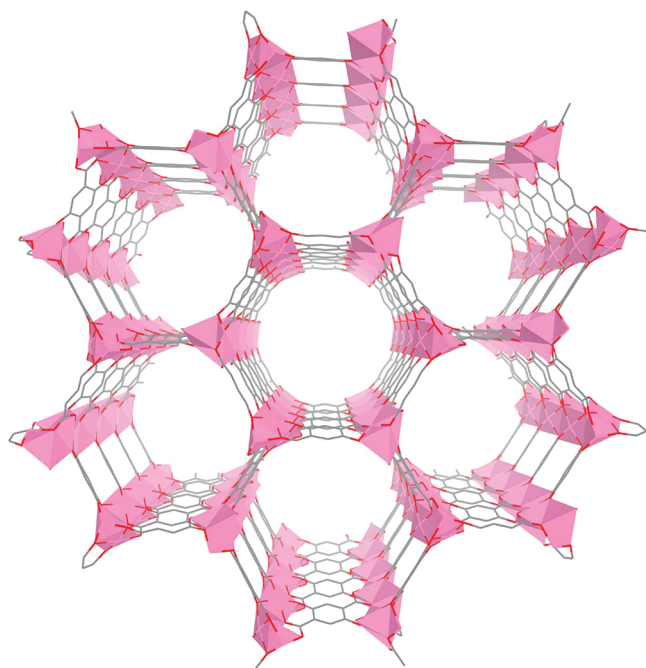


Figure 1. View of the one-dimensional channels present in the M/DOBDC structure. M = Zn, Ni, Co, or Mg; C: gray stick, O: red stick.

capacity under the same conditions. We found that Ni/DOBDC has a higher CO₂ capacity than NaX and 5A zeolites at 0.1 atm and 25 °C. In addition, water does not affect CO₂ adsorption in Ni/DOBDC as much as in NaX and 5A zeolites, and it is much easier to remove water from Ni/DOBDC by regeneration. In other words, Ni/DOBDC can adsorb more CO₂ than traditional zeolites under the same moist conditions. Therefore, Ni/DOBDC is promising for CO₂ capture from flue gas.

Besides having high CO₂ capacities under moist conditions, high stabilities are also critical for the application of MOFs in CO₂ capture from flue gases. However, research on the stability of MOFs is scarce in the literature. Low et al.¹⁸ found that the stability of MOFs in steam correlated with the dissociation energy of the metal–ligand bond, and they generated a steam stability map for several MOFs. Kizzie et al.¹⁹ measured CO₂ saturated capacities for the hydrated DOBDC series of MOFs after regeneration and observed significant decreases in capacities for Mg/DOBDC and Zn/DOBDC compared to the original samples. In order to evaluate the potential of using the DOBDC series of MOFs to capture CO₂ from flue gases, their stabilities toward high temperature water vapor, long-term storage, and trace amounts of acid gases should be addressed as well.

In this paper, as a follow-up to our previous papers,^{17,18} we select Mg/DOBDC and Ni/DOBDC (also known as Mg-MOF-74 and Ni-MOF-74 or CPO-27-Mg and CPO-27-Ni) for stability studies. These have the highest CO₂ capacities at 0.1 atm among the reported MOFs. We investigate their stabilities toward steam conditioning and long-term storage. Simulated flue gas conditioning effects on Ni/DOBDC are studied as well. CO₂ capacity is used throughout as a practical measure of the state of an adsorbent.

2. EXPERIMENTAL SECTION

2.1. Synthesis. The Ni/DOBDC and Mg/DOBDC samples were synthesized at UOP following procedures in the literature.^{15,17,20} Briefly,

for Ni/DOBDC, nickel acetate (18.7 g, 94.0 mmol, Aldrich) and 2,5-dihydroxyterephthalic acid (37.3 g, 150 mmol, Aldrich) were placed in 1 L of mixed solvent consisting of equal parts tetrahydrofuran (THF) and deionized water. The mixture was then put into a 2 L Parr reactor and heated at 110 °C for 3 d. The as-synthesized sample was filtered and washed with water. Then, the sample was dried in air, and the solvent remaining inside the sample was exchanged with ethanol 6 times over 8 d. Finally, the sample was heated under nitrogen and stored in a drybox for later measurements.

For Mg/DOBDC, magnesium nitrate hexahydrate (0.475 g, 1.85 mmol, Fisher) and 2,5-dihydroxyterephthalic acid (0.111 g, 0.559 mmol, Aldrich) was added into a 15:1:1 (v/v/v) mixture of DMF–ethanol–water (50 mL). The suspension was mixed well and then dispensed to five 20-mL Parr reactors. The reactors were capped tightly with Teflon-lined caps and placed in an oven at 125 °C for 20 h. Then, the reactors were removed from the oven and allowed to cool to room temperature. The mother liquor was decanted and replaced with methanol four times over 2 d. The solvent was removed under vacuum at 250 °C over 5 h, yielding the yellow crystalline material. The activated material was stored under vacuum for later use.

2.2. Apparatus and Procedures. In order to assess the stability of the DOBDC series of MOFs as adsorbents for CO₂ capture from flue gas, steam was used to condition the two MOF samples to simulate long-term usage under moist conditions. CO₂ isotherms were measured and compared for the MOF samples before and after the steaming processes. A reactor described in our previous paper¹⁸ was used for the steam conditioning process. The high-throughput heat treatment unit contained 48 parallel heaters arrayed in six rows and eight columns. Steam was generated by combining a liquid source and a gas source inside heated quartz blenders. The steam was delivered by row to 48 quartz tube reactors. MOF materials were loaded into each of the quartz tubes. The materials were regenerated at 150 °C overnight in flowing nitrogen before the steaming process. Steam (nitrogen with 5 mol % water at 100 °C) was introduced for 2 h. Samples were then cooled to room temperature.

Figure 2 shows a schematic diagram of the apparatus that was used in our experiments to study the simulated flue gas conditioning effect. The simulated flue gas used in our experiment was composed of 16% CO₂, 100 ppm SO₂, and 10 ppm NO in N₂. Saturated water vapor at 17 °C was generated using a water sparger and added to the flow of simulated flue gas. Fixed flow rates of water vapor and simulated flue gas were passed through a 0.9 mL adsorption bed loaded with a regenerated MOF sample. Typically, 3 sccm of simulated flue gas and 3 sccm of water vapor in helium were passed through an adsorption bed loaded with Ni/DOBDC at room temperature for 72 h. The conditioning effects of either simulated flue gas or water alone were also studied. CO₂ isotherms were measured for the same sample before and after the simulated flue gas conditioning to reveal the effects of humidity and acid gas conditioning at room temperature on CO₂ adsorption.

All of the MOF samples were regenerated at 150 °C under vacuum for 12 h before isotherm measurements. In the simulated flue gas and water vapor conditioning experiments, the hydrated Ni/DOBDC sample was first subjected to vacuum at room temperature for 2 h to remove most of the adsorbed water and then regenerated at 150 °C under vacuum for 12 h. This procedure can avoid suddenly vaporizing the adsorbed water in Ni/DOBDC, which will damage its structure and thus impact its CO₂ capacity. Our point of interest (POI) was selected to be 0.1 atm CO₂ and 38 °C in this research. The CO₂ partial pressure in flue gas is approximately 0.1 atm, and 38 °C represents a cooled flue gas. All of the isotherm data were measured using a gravimetric system equipped with a Rubotherm balance with a 1 μg accuracy.

Powder X-ray diffraction was used to confirm the crystal structure of the aged DOBDC materials before and after steaming. The spectra were measured using a Scintag X1h/h automated powder diffractometer with

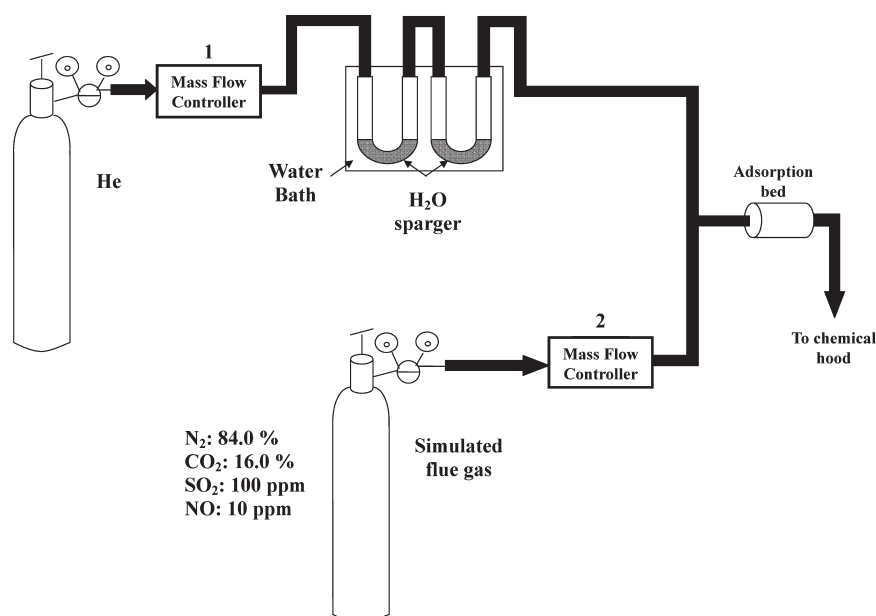


Figure 2. Simulated flue gas conditioning apparatus.

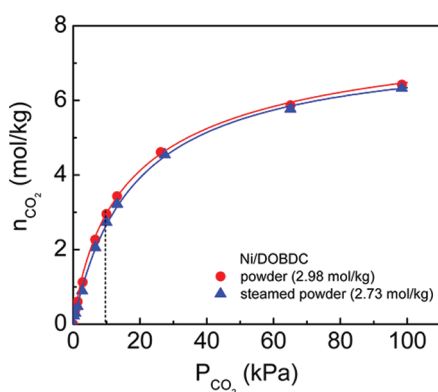


Figure 3. CO₂ isotherms at 38 °C for Ni/DOBDC powder before and after steaming for 2 h. Legend gives capacities at POI.

Cu target, a Peltier-cooled solid-state detector, a zero background Si(5 1 0) support, and with a copper X-ray tube as the radiation source.

Nitrogen adsorption isotherms were measured at -196.1 °C using a Micromeritics ASAP 2020 porosimeter with UHP nitrogen as the analysis gas. Prior to measurement, approximately 0.2 g of each sample was degassed by heating to 90 °C under vacuum to 20 μ bar for 2 h and then heating under vacuum at 150 °C for 12 h. In this way, the regeneration procedure for the materials mirrored that used during CO₂ isotherm measurements.

3. RESULTS AND DISCUSSION

3.1. Stability toward Steaming. The 38 °C CO₂ isotherms for Ni/DOBDC and Mg/DOBDC powder before and after steaming are shown in Figures 3 and 4, respectively. The CO₂ capacity at the POI for the steamed Ni/DOBDC is 2.73 mol/kg. This is very close to that of the unsteamed sample, 2.98 mol/kg. Only a 8.4% loss was found in CO₂ capacity at the POI for the steamed Ni/DOBDC powder.

In contrast to Ni/DOBDC, Mg/DOBDC lost a significant amount of CO₂ capacity after the steaming process. A 51% loss

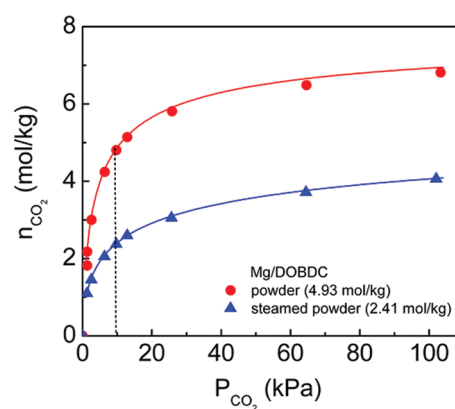


Figure 4. CO₂ isotherms at 38 °C for Mg/DOBDC powder before and after steaming for 2 h. Legend gives capacities at POI.

was found in the CO₂ capacity at the POI for the steamed Mg/DOBDC. Mg/DOBDC has a capacity of 4.93 mol/kg at the POI before steaming, which is much higher than that of Ni/DOBDC. However, the Mg/DOBDC has a lower CO₂ capacity at the POI than Ni/DOBDC after steaming. Therefore, Ni/DOBDC is more stable toward steam conditioning because it retains more CO₂ capacity after steaming.

On the basis of our experience, longer exposure times result in more damage to MOFs. In addition, we used steam at 100 °C with different water vapor concentrations to condition Ni/DOBDC samples synthesized in different batches for 2 h, and the results show that the CO₂ capacities of the steamed Ni/DOBDC samples have low values when the water vapor concentration is above 10% (see Supporting Information Figure S1.)

3.2. Stability toward Storage. Besides the impact on CO₂ capacity caused by steaming, Ni/DOBDC and Mg/DOBDC were also investigated to determine whether they lose CO₂ capacity over time with storage. Samples obtained immediately after synthesis and activation processes are referred to below as fresh samples, and samples that have been stored in sealed

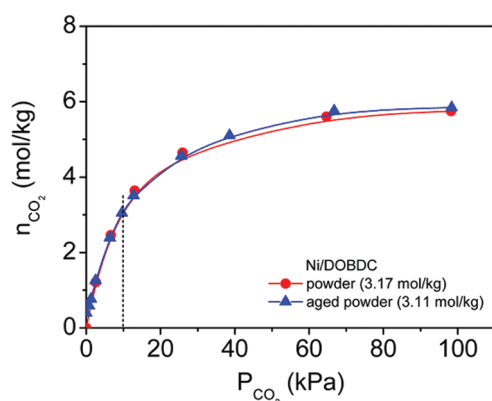


Figure 5. CO₂ isotherms at 38 °C for fresh and aged Ni/DOBDC powders. Legend gives capacities at POI.

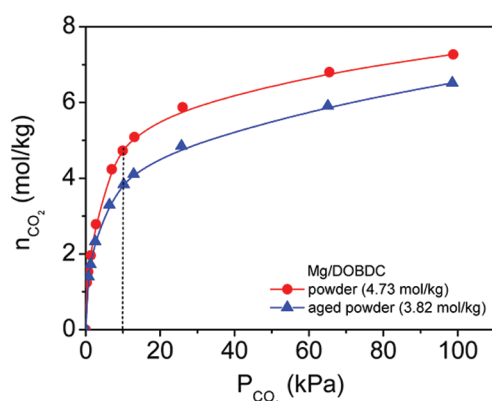


Figure 6. CO₂ isotherms at 38 °C for fresh and aged Mg/DOBDC powders. Legend gives capacities at POI.

containers for approximately one year are referred to as aged samples. CO₂ isotherms were measured and compared for the fresh and aged samples.

The 38 °C CO₂ isotherms for the fresh and aged Ni/DOBDC powders are shown in Figure 5. The results show that Ni/DOBDC can maintain its CO₂ capacity, which is about 3.1 mol/kg at the POI, after aging. The CO₂ capacities at the POI for the Ni/DOBDC used in this study and the Ni/DOBDC used in the steaming study varied slightly because they were from different synthesis batches.

The 38 °C CO₂ isotherms for the fresh and aged Mg/DOBDC powders are compared in Figure 6. The CO₂ capacities at the POI for the Mg/DOBDC used in this study and the Mg/DOBDC used in the steaming study varied slightly also because they were from different synthesis batches. The CO₂ capacity at the POI for the aged Mg/DOBDC decreased by about 22.6% compared with the fresh sample, even though the sample had been sealed in its original container and stored inside a desiccator. A longer storage time may cause an even larger decrease in the CO₂ capacity at the POI for Mg/DOBDC.

3.3. Physical Properties and Stability. Powder X-ray diffraction was run on the aged and steamed samples to determine whether the changes in CO₂ capacity are related to crystal structure (see Supporting Information Figure S2). After steaming, the Mg/DOBDC crystal structure remains intact; however, the crystal structure of the steamed, aged Ni/DOBDC breaks

Table 1. BET Surface Areas for Mg/DOBDC and Ni/DOBDC^a

sample	BET surface area (m ² /g)		
	fresh	aged	steamed
Mg/DOBDC	1406	425	38
Ni/DOBDC	922	784	6

^a Note: Surface areas for the fresh samples were measured at the time of synthesis by UOP. Aged samples were tested using a different Micromeritics ASAP 2020 adsorption analyzer at Vanderbilt University. Surface areas for the steamed samples were obtained at Vanderbilt after about 1 year of storage.

down. Kizzie et al.¹⁹ have reported that the CO₂ capacity of Mg/DOBDC drops significantly after water adsorption processes followed by thermal regeneration, despite its seemingly intact crystal structure. In our study, Mg/DOBDC exhibits a large drop in capacity, even though the XRD results show that the steamed sample remains largely structured. Therefore, CO₂ capacities at subatmospheric pressures are not related with the crystallinities of these MOF samples. Instead, they should depend on the density of the UMCs in the MOFs.^{11,17}

Nitrogen isotherms were also measured on these samples to see if there is a correlation between surface area and CO₂ capacity. In both instances, the surface areas for the steamed, aged samples are lower than those of the unsteamed, aged samples. Table 1 compares surface areas for the fresh, aged, and steamed samples. It is evident that, after steaming, the crystal structure of the aged Ni/DOBDC sample breaks down, resulting in a decrease in surface area. For the aged Mg/DOBDC, the crystal structure remains intact according to XRD; however, there is an obvious drop in surface area after long-term storage. In addition, the Ni/DOBDC lost less surface area after long-term storage compared with the Mg/DOBDC, which indicates again that the Ni/DOBDC is more stable as determined by CO₂ adsorption.

According to a comparison of CO₂ capacities and surface areas, Ni/DOBDC is more stable than Mg/DOBDC. One possible explanation is that Mg is a stronger reducing agent than Ni. The standard reduction potential for Ni²⁺ is −0.26 eV, while the standard reduction potential for Mg²⁺ is −2.37 eV.²¹ Therefore, the Mg in Mg/DOBDC is more prone to react with water or oxygen in air, which would lead to a decrease in the density of the UMCs.

On the basis of the standard reduction potentials of the four metal ions common to the DOBDC series of MOFs, Zn²⁺ (−0.76 eV), Ni²⁺ (−0.26 eV), Co²⁺ (−0.28 eV), and Mg²⁺ (−2.37 eV), the sequence for the stability of the series is Ni ≈ Co > Zn > Mg/DOBDC. This result is similar to the trend of the percentages of recovered CO₂ capacities for the DOBDC series of MOFs reported in the literature in which recovered CO₂ capacities were measured for the fully hydrated DOBDC series of MOFs after regeneration.¹⁹ Thus, it appears that, within the DOBDC series, MOFs having metal centers that are weaker reducing agents have smaller changes in capacity than MOFs having metal centers that are stronger reducing agents.

When comparing these MOFs to other commercial adsorbents, the overall stability of the DOBDC series of MOFs does not appear to be as good as that of many of the zeolites. We have been able to achieve almost the same CO₂ isotherm for fresh SA zeolite and SA zeolite that has been stored for more than one year. In addition, we performed a similar steam conditioning

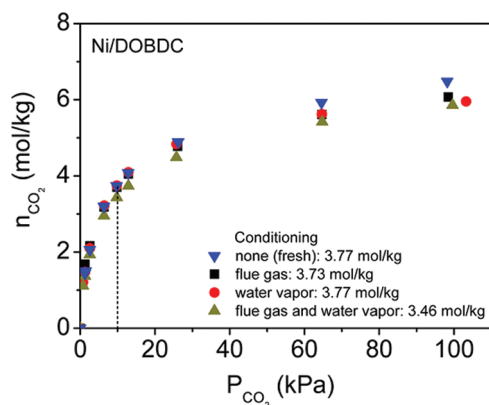


Figure 7. CO₂ isotherms at 25 °C for Ni/DOBDC powder before and after simulated flue gas and water vapor conditioning. The flow rate for both the flue gas and water vapor is 3 sccm, and the water vapor is in helium at 80% RH.

experiment on 13X zeolite and found no change in the crystal structure (see Supporting Information Figure S3), which indicates that 13X zeolite is more stable than the two MOFs we studied in this paper.

3.4. Stability toward Simulated Flue Gas and Humidity. In the envisioned application, there will be direct contact between the adsorbents and the acid gases contained in flue gas. Therefore, it is important for the potential MOF adsorbents to be stable in the presence of acid gases. Ni/DOBDC was selected for the simulated flue gas conditioning study because it is more stable than Mg/DOBDC, as shown in the previous section. CO₂ isotherms were measured at 25 °C for Ni/DOBDC samples before and after conditioning with simulated flue gas to reveal the effects of acid gases and humidity on CO₂ adsorption performance. The simulated flue gas contained a trace amount of SO₂ and NO, and its composition was chosen based on the composition of typical flue gas.

The 25 °C CO₂ isotherm results for Ni/DOBDC powder after different conditioning treatments are shown in Figure 7. Generally, the CO₂ capacities at 0.1 atm and 25 °C for Ni/DOBDC powder did not change significantly after being conditioned with different simulated flue gases and water vapor at room temperature (note the numerical values shown in the figure for the CO₂ loadings at 0.1 atm). We did not observe a substantial decrease in CO₂ capacity for the Ni/DOBDC after water vapor conditioning at room temperature as reported in the literature.¹⁹ One explanation for this is that in our slow regeneration procedure, we avoided suddenly vaporizing the adsorbed water in the Ni/DOBDC which could significantly impact its CO₂ capacity. Flue gas conditioning at room temperature only slightly affected CO₂ adsorption in Ni/DOBDC. Acid gas molecules do not react extensively with the metal sites in Ni/DOBDC at room temperature. However, moisture can impact the simulated flue gas conditioning effect on CO₂ adsorption in Ni/DOBDC, as indicated by the reduced capacity of 3.46 mol/kg at 0.1 atm. This reduction may be due to the increase in the acidity of the solution formed by the dissolution of acid gases in water. Thus, the H⁺ formed from the reactions between the acid gases (SO₂ and NO) and water can break the coordination bonds between metal atoms and oxygen atoms, thereby reducing the density of UMCs in Ni/DOBDC. However, since the simulated flue gas contains only trace amounts (ppm levels) of SO₂ and NO, the concentration of

H⁺ is so small that only a slight change in CO₂ capacity was observed after the Ni/DOBDC was treated with both the simulated flue gas and water vapor at room temperature.

4. CONCLUSIONS

The two most promising of the DOBDC series of MOFs based on prior measurements, Ni/DOBDC and Mg/DOBDC, were synthesized, and the stability effects on CO₂ adsorption were studied. Mg/DOBDC is less stable than Ni/DOBDC because Mg is more easily oxidized, which reduces the density of UMCs in the material. Within the DOBDC series, MOFs having less reductive metal centers appear to be more stable to changes in CO₂ capacity than those having more reductive metal centers in their structures. Ni/DOBDC can maintain its CO₂ capacity after steaming and long-term storage, while Mg/DOBDC loses a significant amount of its CO₂ capacity. Conditioning with dry simulated flue gas at room temperature only slightly affected CO₂ adsorption in Ni/DOBDC, but water vapor enhanced the impact of this effect. Ni/DOBDC has large and relatively stable capacities at subatmospheric pressures for CO₂ capture from flue gas.

■ ASSOCIATED CONTENT

S Supporting Information. Additional CO₂ isotherms for Ni/DOBDC powder conditioned at different water vapor concentrations. XRD patterns for Ni/DOBDC, Mg/DOBDC, and 13X zeolite. This material is available free of charge via the Internet at <http://pubs.acs.org>.

■ AUTHOR INFORMATION

Corresponding Author

*Fax: (615) 343-7951. E-mail address: m.douglas.levan@vanderbilt.edu (M. D. LeVan).

■ ACKNOWLEDGMENT

This project was supported by the U.S. Department of Energy through the National Energy Technology Laboratory under Award No. DE-FC26-07NT43092. However, any opinions, findings, conclusions, or recommendations expressed herein are those of the authors and do not necessarily reflect the views of the DOE. We thank Professor Adam Matzger at the University of Michigan for providing a diagram of the DOBDC series of MOFs (Figure 1).

■ REFERENCES

- (1) Mueller, U.; Schubert, M.; Teich, F.; Puetter, H.; Schierle-Arndt, K.; Pastre, J. *J. Mater. Chem.* **2006**, *16*, 626–636.
- (2) Walton, K. S.; Millward, A. R.; Dubbeldam, D.; Frost, H.; Low, J. J.; Yaghi, O. M.; Snurr, R. Q. *J. Am. Chem. Soc.* **2008**, *130*, 406–407.
- (3) Li, H.; Eddaoudi, M.; O’Keeffe, M.; Yaghi, O. M. *Nature* **1999**, *402*, 276–279.
- (4) Chae, H. K.; Siberio-Perez, D. Y.; Kim, J.; Go, Y.; Eddaoudi, M.; Matzger, A. J.; O’Keeffe, M.; Yaghi, O. M. *Nature* **2004**, *427*, 523–527.
- (5) Kitagawa, S.; Kitaura, R.; Noro, S. *Angew. Chem., Int. Ed.* **2004**, *43*, 2334–2375.
- (6) Rowsell, J. L. C.; Millward, A. R.; Park, K. S.; Yaghi, O. M. *J. Am. Chem. Soc.* **2004**, *126*, 5666–5667.
- (7) Rowsell, J. L. C.; Yaghi, O. M. *J. Am. Chem. Soc.* **2006**, *128*, 1304–1315.
- (8) Eddaoudi, M.; Kim, J.; Rosi, N.; Vodak, D.; Wachter, J.; O’Keeffe, M.; Yaghi, O. M. *Science* **2006**, *295*, 469–472.

- (9) Ma, S. Q.; Sun, D. F.; Simmons, J. M.; Collier, C. D.; Yuan, D. Q.; Zhou, H. C. *J. Am. Chem. Soc.* **2008**, *130*, 1012–1016.
- (10) Millward, A. R.; Yaghi, O. M. *J. Am. Chem. Soc.* **2005**, *127*, 17998–17999.
- (11) Yazaydin, A. O.; Snurr, R. Q.; Park, T. H.; Koh, K.; Liu, J.; LeVan, M. D.; Benin, A. I.; Jakubczak, P.; Lanuza, M.; Galloway, D. B.; Low, J. J.; Willis, R. R. *J. Am. Chem. Soc.* **2009**, *131*, 18198–18199.
- (12) Britt, D.; Furukawa, H.; Wang, B.; Glover, T. G.; Yaghi, O. M. *Proc. Natl. Acad. Sci. U.S.A.* **2009**, *106*, 20637–20640.
- (13) Bao, Z. B.; Yu, L.; Ren, Q. L.; Lu, X. Y.; Deng, S. G. *J. Colloid Interface Sci.* **2011**, *353*, 549–556.
- (14) Rosi, N. L.; Kim, J.; Eddaoudi, M.; Chen, B. L.; O’Keeffe, M.; Yaghi, O. M. *J. Am. Chem. Soc.* **2005**, *127*, 1504–1518.
- (15) Caskey, S. R.; Wong-Foy, A. G.; Matzger, A. J. *J. Am. Chem. Soc.* **2008**, *130*, 10870–10871.
- (16) Keskin, S.; Van Heest, T. M.; Sholl, D. S. *ChemSusChem* **2010**, *3*, 879–891.
- (17) Liu, J.; Wang, Y.; Benin, A. I.; Jakubczak, P.; Willis, R. R.; LeVan, M. D. *Langmuir* **2010**, *26*, 14301–14307.
- (18) Low, J. J.; Benin, A. I.; Jakubczak, P.; Abrahamian, J. F.; Faheem, S. A.; Willis, R. R. *J. Am. Chem. Soc.* **2009**, *131*, 15834–15842.
- (19) Kizzie, A. C.; Wong-Foy, A. G.; Matzger, A. J. *Langmuir* **2011**, DOI:10.1021/la200547k.
- (20) Dietzel, P. D. C.; Panella, B.; Hirscher, M.; Blom, R.; Fjellvag, H. *Chem. Commun* **2006**, *9*, 959–961.
- (21) Moore, J. T.; Langley, R. H. *Chemistry 2008–2009*; McGraw-Hill: New York, NY, 2008.